

Optical Absorption of $Y_3Al_5O_{12}$ from 10- to 55 000- cm^{-1} Wave Numbers*

GLEN A. SLACK, D. W. OLIVER, R. M. CHRENKO, AND S. ROBERTS
General Electric Research and Development Center, Schenectady, New York 12302
 (Received 9 August 1968)

The optical absorption coefficient of synthetic single crystals of the garnet $Y_3Al_5O_{12}$ has been measured from photon wave numbers of 10 to 55 000 cm^{-1} at 300°K. The wave-number range 10 to 900 cm^{-1} has been studied at 4°K. The 17 theoretically predicted absorption peaks of the $Y_3Al_5O_{12}$ lattice at 300°K have been found at wave numbers of 123, 163, 223, 255, 293, 332, 373, 395, 430, 457, 510, 530, 570, 690, 722, 784, and 830 cm^{-1} . The fourteenth, fifteenth, and sixteenth peaks are believed to be associated with the $\bar{\nu}_3$ vibrations of the AlO_4 groups in the lattice. The multiphonon lattice absorption bands extend upward to 2400 cm^{-1} wave numbers. Beyond 2400 cm^{-1} the crystal is transparent, with an absorption coefficient $<0.1 cm^{-1}$ up to $\bar{\nu}=30\,000 cm^{-1}$. From 30 000 to 52 000 cm^{-1} the absorption appears to be dominated by trace impurities. The optical absorption increases rapidly for wave numbers above 52 000 cm^{-1} and reaches an absorption coefficient of $10^{+8} cm^{-1}$ at 54 300 cm^{-1} wave numbers (6.73 eV or 1840 Å). Some comments are also made on the relationship of the lattice modes of yttrium aluminum garnet (YAG) to the phonon sidebands of electronic transitions of impurity ions in YAG.

INTRODUCTION

THE synthetic, nonmagnetic garnet $Y_3Al_5O_{12}$, YAG, is a prototype material for many other magnetic garnets such as $Y_3Fe_5O_{12}$ and $Dy_3Al_5O_{12}$. It is a transparent, cubic solid, and single crystals can be grown from the melt.¹⁻⁴ In the present studies we have examined the optical absorption of single crystals of YAG grown in this laboratory by techniques similar to those already published.^{1,3,4} These studies were made at photon wave numbers $\bar{\nu}$ in the region $10 \leq \bar{\nu} \leq 55\,000 cm^{-1}$ (wavelengths of 1000 to 0.18 μ) in order to study both the lattice bands between 120 and 2500 cm^{-1} and the region of the fundamental absorption edge at 50 000 cm^{-1} wave numbers. One impetus for this work came from a desire to understand the behavior of the lattice phonons as they affect the thermal conductivity⁵⁻⁷ and the ultrasonic attenuation^{5,7-9} of the crystals. The other impetus came from a desire to understand the optical absorption spectra of the chemical impurities and transition-metal ions¹⁰⁻¹⁷ as

well as various rare-earth ions¹⁸⁻³¹ dissolved in host crystals of YAG or other garnets. This becomes particularly important when studying the rare-earth ions because many of the energy levels of the ground-state manifold of the rare-earth ions lie in the region of the lattice bands.

Several previous studies of some of the optical properties of pure, undoped YAG have been made. These can be divided into studies in the infrared^{2,3,11} and ultraviolet^{2,3,32} spectral regions. Some refractive index measurements in the near infrared and visible have also been made,³³ and a comment that there are no lattice absorption peaks in YAG for photon wave numbers less than 80 cm^{-1} also exists.³⁴

Belyaev, *Opt. i Spektroskopiya* **19**, 817 (1965) [English transl.: *Opt. Spectry. (USSR)* **19**, 451 (1965)].

¹⁵ O. Schmitz-Dumont, *Bull. Soc. Chim. France*, p. 1099 (1965).

¹⁶ M. J. Taylor, *Proc. Phys. Soc. (London)* **90**, 487 (1967).

¹⁷ D. L. Wood and J. P. Remeika, *J. Chem. Phys.* **46**, 3595 (1967).

¹⁸ L. G. Van Uitert, R. C. Linares, and A. A. Ballman, *J. Chem. Phys.* **36**, 702 (1962).

¹⁹ E. Y. Wong, O. M. Stafudd, and D. R. Johnston, *J. Chem. Phys.* **36**, 702 (1962).

²⁰ D. L. Wood, *J. Chem. Phys.* **39**, 1671 (1963).

²¹ J. A. Koningstein and J. E. Geusic, *Phys. Rev.* **136**, A711 (1964).

²² J. A. Koningstein, *Phys. Rev.* **136**, A717 (1964).

²³ J. A. Koningstein and J. E. Geusic, *Phys. Rev.* **136**, A726 (1964).

²⁴ J. A. Koningstein, *Theoret. Chim. Acta* **3**, 271 (1965).

²⁵ G. A. Bogomolova, A. A. Kaminskii, and V. A. Timofeeva, *Phys. Status Solidi* **16**, 165 (1966).

²⁶ W. W. Holloway and M. Kestigian, *Phys. Letters* **21**, 364 (1966).

²⁷ F. N. Hooge, *J. Chem. Phys.* **45**, 4504 (1966).

²⁸ J. A. Koningstein, *J. Chem. Phys.* **44**, 3957 (1966).

²⁹ J. A. Koningstein, *Theoret. Chim. Acta* **5**, 327 (1966).

³⁰ R. A. Buchanan, K. A. Wickersheim, J. J. Pearson, and G. F. Herrmann, *Phys. Rev.* **159**, 245 (1967).

³¹ J. J. Pearson, G. F. Herrmann, and R. A. Buchanan, *J. Appl. Phys.* **39**, 980 (1968).

³² M. Bass and A. E. Paladino, *J. Appl. Phys.* **38**, 2706 (1967).

³³ W. L. Bond, *J. Appl. Phys.* **36**, 1674 (1965).

³⁴ R. C. Milward, *Phys. Letters* **25A**, 19 (1967).

* Supported in part by the U. S. Air Force Materials Laboratory, Wright-Patterson Air Force Base, under Contract No. F33615-67C-1399.

¹ R. C. Linares, *Solid State Commun.* **2**, 229 (1964).

² H. M. O'Bryan and P. B. O'Connor, *Bull. Am. Ceram. Soc.* **45**, 578 (1966).

³ B. Cockayne, *J. Am. Ceram. Soc.* **49**, 204 (1966); see Fig. 5.

⁴ W. Bardsley and B. Cockayne, *J. Phys. Chem. Solids*, *Suppl.* **1**, 109 (1967).

⁵ D. W. Oliver and G. A. Slack, *J. Appl. Phys.* **37**, 1542 (1966).

⁶ P. H. Klein and W. J. Croft, *J. Appl. Phys.* **38**, 1063 (1967).

⁷ M. G. Holland, *IEEE Trans. Sonics Ultrasonics* **SU-15**, 18 (1968).

⁸ E. M. Gyorgy, M. D. Sturge, D. B. Fraser, and R. C. LeCraw, *Phys. Rev. Letters* **15**, 19 (1965).

⁹ M. G. Holland, A. E. Paladino, and R. W. Bierig, *J. Appl. Phys.* **38**, 4100 (1967).

¹⁰ K. A. Wickersheim, R. A. Lefever, and B. M. Hanking, *J. Chem. Phys.* **32**, 271 (1960).

¹¹ K. A. Wickersheim, *J. Appl. Phys.* **32**, 2055 (1961).

¹² D. L. Wood, J. Ferguson, K. Knox, and J. F. Dillon, Jr., *J. Chem. Phys.* **39**, 890 (1963).

¹³ G. Burns, E. A. Geiss, B. A. Jenkins, and M. I. Nathan, *Phys. Rev.* **139**, A1687 (1965).

¹⁴ P. P. Feofilov, V. A. Timofeeva, M. N. Tolstoi, and L. M.

SAMPLES

The samples used in the present study were prepared from single crystals of YAG that were grown in this laboratory from the melt^{1,3,4} in an iridium crucible in an inert or slightly oxidizing atmosphere. High purity (99.999%) Y_2O_3 powder³⁵ and single crystals of Al_2O_3 ³⁶ were used as the starting material. Chemical analyses indicated that typical impurity concentrations of the grown crystals were 2 ppm by weight of Ir, and less than 10 ppm by weight of Ca, Cu, Fe, Mg, Na, Ni, and Si. The Ir came from the iridium crucible, and the concentration in the crystals varied somewhat from run to run. The total impurity content of the crystals was, therefore, probably in the range of 10 to 100 ppm.

These crystals were cut with a diamond wheel into flat slabs and were polished to an optical finish with Al_2O_3 abrasives. The crystals studied ranged from 1 to 10^{-3} cm in thickness. This range of thickness allowed us to measure the optical absorption coefficient α from 10^{-1} to $5 \times 10^{+3}$ cm^{-1} . The fact that the crystal is cubic means that the optical absorption coefficient α is isotropic. Hence no special care was needed with regard to the crystallographic orientation of the samples. For the highest range of α values from 5×10^3 to 2×10^4 cm^{-1} the measurements were made on YAG powder prepared from crushing a single crystal. The powder was mixed into KBr powder with a 1:20 volume ratio and was compressed into a disk 0.08 cm thick. The absolute α values for these disks were estimated by matching a few of the weaker absorption peaks to those for the thinnest single crystal.

APPARATUS

The measurements from $10 < \bar{\nu} < 200$ cm^{-1} were made with a grating spectrometer previously described.³⁷ The measurements from 200 to 4000 cm^{-1} were made with a Beckman³⁸ IR12 grating spectrophotometer, while those from 4000 to 55 000 cm^{-1} were made with a Cary³⁹ model 14 recording spectrophotometer.

RESULTS

The curves in Fig. 1 show the optical absorption coefficient α for YAG for photon wave numbers $50 \leq \bar{\nu} \leq 400$ cm^{-1} at temperatures of 300° and 4°K (i.e., 4 to 6°K). The results for 77°K were found to be nearly the same as those for 4°K in the range $200 < \bar{\nu} < 3000$ cm^{-1} , and are not shown. No absorption was detected from 10 to 50 cm^{-1} . The coefficient α was determined from

$$I = I_0(1 - R)^2 e^{-\alpha t}, \quad (1)$$

where I and I_0 are transmitted and incident light

³⁵ Rare-Earth Division, American Potash and Chemical Corp., West Chicago, Ill.

³⁶ Crystal Products Department, Electronics Division, Union Carbide Corporation, Boston, Mass.

³⁷ S. Roberts and D. D. Coon, J. Opt. Soc. Am. **52**, 1023 (1962).

³⁸ Beckman Instruments Inc., Fullerton, Calif.

³⁹ Applied Physics Corporation, Monrovia, Calif.

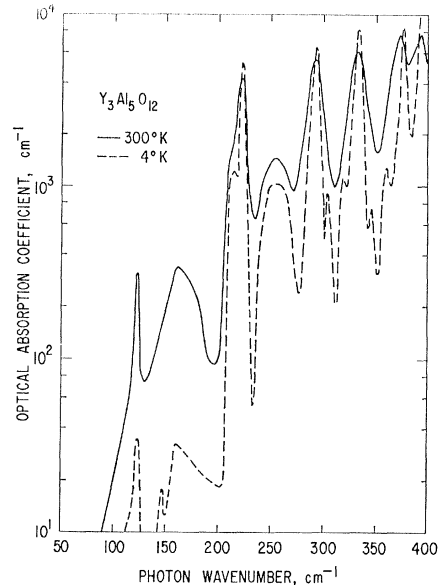


FIG. 1. The optical absorption coefficient α versus photon wave number $\bar{\nu}$ for $Y_3Al_5O_{12}$ at 4 and 300°K. The spectrometer resolution for $\bar{\nu}$ is about 4 cm^{-1} .

intensity, R is the single-surface reflection loss at normal incidence, and t is the sample thickness. Note that the absorption lines sharpen somewhat on cooling, and that some of the weaker lines are resolvable at 4°K. A list of the various absorption peaks is given in Table I. The lowest-energy absorption peak was found at $\bar{\nu} = 123$ cm^{-1} .

Figure 2 shows the whole lattice band region from 0 to 2400 cm^{-1} at a temperature of 300°K. The absorption coefficient was carefully measured not only in the highly absorbing region for $100 < \bar{\nu} < 860$ cm^{-1} , but also in the region of decreasing absorption from 860 $cm^{-1} < \bar{\nu} < 2400$ cm^{-1} . As will be shown later, this latter region is believed to be dominated by two-phonon and three-phonon absorption processes. The region of Fig. 2 from $400 < \bar{\nu} < 860$ cm^{-1} was also studied at 4°K, but very little difference was found between these results and those shown in Fig. 2 for 300°K. The one new peak found at 4°K is given in Table I along with some estimates of the intensities of the absorption bands.

There is a region of very low-absorption coefficient where $\alpha < 0.1$ cm^{-1} from $2400 < \bar{\nu} < 30\ 000$ cm^{-1} . This region produces an "optical window" from wavelengths of 0.33 μ in the ultraviolet to 4.2 μ in the near infrared. The YAG crystals are therefore clear, transparent, and colorless to the eye. The optical absorption between $30\ 000 < \bar{\nu} < 55\ 000$ cm^{-1} is shown in Fig. 3. Here the absorption curves at low values of α are seen to vary from sample to sample. The descriptions of the various crystals are given in Table III.

DISCUSSION OF THE RESULTS

In order to understand the results it is useful to know the crystal structure of $Y_3Al_5O_{12}$. It is a body-

TABLE I. Optical absorption peaks in $Y_3Al_5O_{12}$ in the one-phonon region at 300° and 4°K.

300°K				4°K	
Present work		Wickersheim ^a		Present work	
$\bar{\nu}^b$	α^c	$\bar{\nu}$	Strength ^d	$\bar{\nu}$	Strength ^{e,d}
cm ⁻¹	cm ⁻¹	cm ⁻¹		cm ⁻¹	cm ⁻¹
123	3.1E2			123	3.4E1
				148	1.8E1
163	3.4E2			160	3.3E1
				215	1.2E3
223	4.2E3			223	5E3
255	1.5E3			255	1.0E3
293	5.5E3			293	6E3
				305	9.0E2
				320	1.1E3
332	6E3	330	m	333	8E3
				346	7.4E2
				361	1.3E3
373	8E3	370	w	377	~8E3
395	8E3	395	w	397	~1E4
430	9E3	430	m	436	s
457	1E4	460	s	463	vs
510	6E3	510	w	516	m
530	5E3	535	w	535	w (shl on 516)
570	6E3	570	m	572	m
690	1E4	690	s	700	s
722	8E3	720	s	729	s
				760	w (shl on 729)
784	7E3	800	m	792	s
830	5E3	835	w	820	m (shl on 792)

^a See Ref. 11.

^b The $\bar{\nu}$ values for the peaks are believed to be accurate to ± 3 cm⁻¹.

^c The α values at the peaks in the α versus $\bar{\nu}$ curves are given in units of cm⁻¹. The E means the exponent of ten. Thus an α of 310 cm⁻¹ is 3.1×10^2 cm⁻¹ or 3.1E2.

^d Where α at the peak was not measured explicitly the absorption is listed as either strong (s), medium (m) or weak (w). If one band appears as a shoulder on the side of another it is listed as shl.

centered cubic crystal^{40,41} with a lattice constant of 12.00 Å, and contains eight formula groups or 160 atoms in this unit cell. The Y³⁺ ions are surrounded by eight oxygen ions in a dodecahedral site, 40% of the Al³⁺ ions are surrounded by six oxygen ions in a distorted octahedral site, and 60% of the Al³⁺ ions are surrounded by four oxygen ions in a distorted tetrahedral site. The shortest cation-anion separation occurs for the tetrahedral site where the Al-O distance⁴¹ is 1.76 Å. The octahedral Al-O distance is 1.94 Å, while the Y-O distance averages 2.37 Å.

The YAG crystals are synthetic versions of the natural garnets which are all orthosilicates.⁴² This means that the SiO₄ groups in the natural garnets and the AlO₄ groups in YAG are all isolated from one another. Hence one can consider with some justification that these AlO₄ groups act as separate, isolated molecular units in the lattice. Thus these groups may give rise to what are termed⁴³ internal modes of the lattice. There will also be other⁴³ external or lattice modes involving the lattice as a whole. The total number of modes of the crystal depends on the number of atoms

⁴⁰ S. Geller and M. A. Gilleo, *J. Phys. Chem. Solids* 3, 30 (1957).

⁴¹ F. Euler and J. A. Bruce, *Acta Cryst.* 19, 971 (1965).

⁴² W. A. Deer, R. A. Howie, and J. Zussman, *Rock Forming Minerals* (John Wiley & Sons, Inc., New York, 1962), Vol. 1, p. 77.

⁴³ A. S. Davydov, *Theory of Molecular Excitons* (McGraw-Hill Book Co., New York, 1962), Chap. 1.

per unit cell. The standard crystallographic unit cell of YAG is a body-centered cube with $a_0=12.00$ Å and contains eight molecules of $Y_3Al_5O_{12}$. The primitive unit cell or the cellular polyhedron⁴⁴ of the body-centered cubic lattice is a tetradecahedron of 14 sides and contains only four molecules of $Y_3Al_5O_{12}$. This cell contains 80 atoms or 240 possible normal modes of vibration. A group-theoretical analysis⁴⁵ of these normal modes indicates that there are only 17 possible modes which are infrared-active, and these are all T_{1u} modes. The complete identification of which mode is which would be a tedious process, and will not be attempted here. However, some degree of analysis is possible.

One-Phonon Region

The wave number region $0 < \bar{\nu} < 860$ cm⁻¹ in Fig. 2 is labeled the one-phonon region where the absorption of one photon generates one phonon. It is given this assignment since the α values in this region are all fairly high and then rapidly decrease for $\bar{\nu} > 860$ cm⁻¹. Furthermore the highest mode at $\bar{\nu}=835$ cm⁻¹ lies about at the energy expected, as will be shown. With this limit to the one-phonon region the 300°K spectrum in Fig. 2 shows just 17 peaks, the number predicted

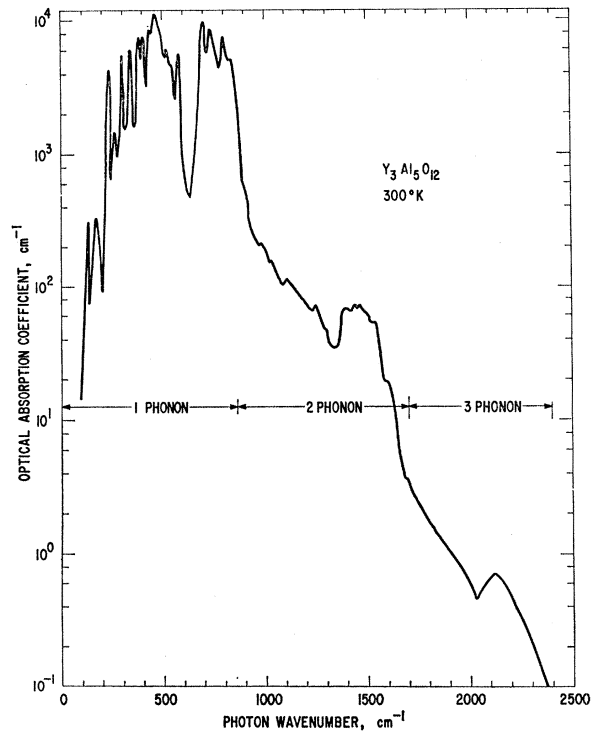


Fig. 2. The optical absorption coefficient α versus photon wave number $\bar{\nu}$ for $Y_3Al_5O_{12}$ at 300°K in the infrared. The spectrometer resolution for $\bar{\nu}$ is about 4 cm⁻¹.

⁴⁴ F. Seitz, *Modern Theory of Solids* (McGraw-Hill Book Co., New York, 1940), p. 331.

⁴⁵ M. C. M. O'Brien, Oxford University (private communication).

from the group theory. These can be compared with the results of Wickersheim¹¹ on powdered YAG at 300°K (see Table I). The agreement both with respect to α and $\bar{\nu}$ is good in the region of overlap $330 < \bar{\nu} < 835$ cm^{-1} . The 4°K spectrum in Fig. 1 and Table I also shows seven weaker peaks ($\bar{\nu}=148$, and 215 cm^{-1} , etc.) that are about $\Delta\bar{\nu}=12$ cm^{-1} away from one of the 17 main peaks. Though not present at 300°K these same small satellite peaks are present in the absorption spectrum at 77°K (which is not shown here). Their cause is unclear. They are not caused by crystallographic distortions in YAG since it appears to remain cubic on cooling to low temperatures.⁴⁶ These small peaks may be weak absorptions of some of the 186 other normally infrared-forbidden modes of the lattice. For example, Kravitz⁴⁷ has studied the Raman spectrum of YAG at 300°K and has seen at least 16 Raman modes

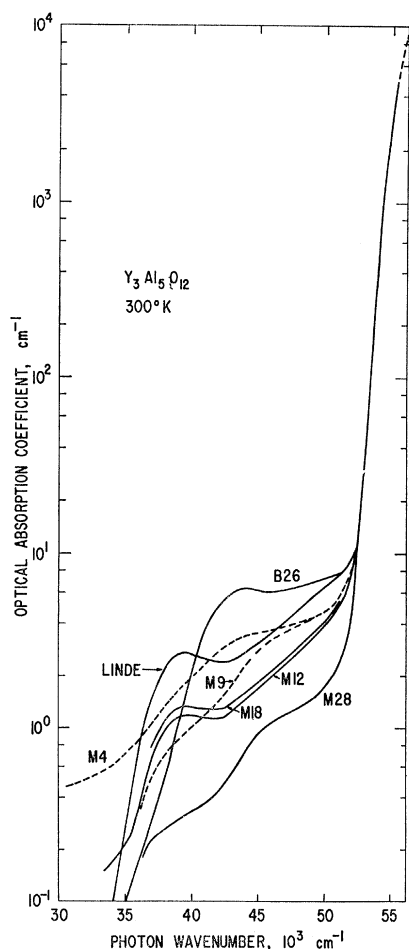


FIG. 3. The optical-absorption coefficient α versus photon wave number $\bar{\nu}$ for several single crystals of $Y_3Al_5O_{12}$ at 300°K in the ultraviolet region. The spectrometer resolution for $\bar{\nu}$ is about 50 cm^{-1} . The curve for M_{15} falls between those for M_{12} and M_{18} , and is therefore not plotted.

⁴⁶ W. J. Croft, *Am. Mineralogist* **50**, 1634 (1965).

⁴⁷ L. C. Kravitz (private communication).

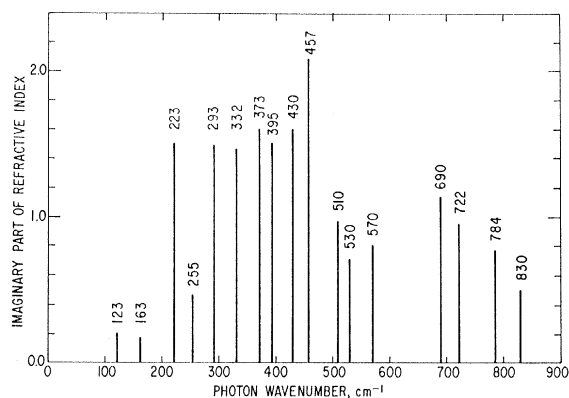


FIG. 4. The imaginary part of the refractive index versus wave number at the absorption maxima for the 17 infrared-active lattice modes of YAG.

that are normally infrared-inactive extending from $165 < \bar{\nu} < 780$ cm^{-1} .

We conclude that the infrared absorption spectrum shows the 17 modes that are expected plus some weak satellites. In Fig. 4 these 17 infrared-active modes are plotted in a k versus $\bar{\nu}$ graph, where the imaginary part of the refractive index k at each absorption peak is related to the absorption coefficient α at the peak by

$$k = 4\pi\alpha/\bar{\nu}. \quad (2)$$

Further identification of the 17 main modes depends on comparing the spectrum of YAG with those of other crystals. Studies^{48,49} of the infrared spectra of various rare-earth oxides (R_2O_3) show that their lattice bands generally occur for $\bar{\nu} < 650$ cm^{-1} . Studies⁵⁰⁻⁵² of octahedrally coordinated Al in Al_2O_3 show that the six infrared absorption bands occur for $383 < \bar{\nu} < 640$ cm^{-1} . The tetrahedrally coordinated AlO_4 groups in crystals have been found⁵³ to have a characteristic absorption for $720 < \bar{\nu} < 780$ cm^{-1} . Similarly $[Al(OH)_4]^-$ molecular groups in solution have been found⁵⁴ to have characteristic infrared-active modes at $\bar{\nu}_3 = 720$ cm^{-1} , $\bar{\nu}_4 = 300$ cm^{-1} . In Fig. 2 we see that the spectrum divides nicely into two groups of absorption bands. The lower group is $0 < \bar{\nu} < 620$ cm^{-1} and the higher one is $620 < \bar{\nu} < 860$ cm^{-1} . Thus it seems reasonable to conclude that the higher group $620 < \bar{\nu} < 860$ cm^{-1} is a characteristic absorption of only the AlO_4 groups in the YAG lattice. This assignment is further strengthened by comparison of the $620 < \bar{\nu} < 860$ cm^{-1} region of Fig. 2 with the SiO_4 absorption bands in the natural almandine garnet^{10,55} for $970 < \bar{\nu} < 870$ cm^{-1} and the same bands of Si im-

⁴⁸ W. L. Baun and N. T. McDevitt, *J. Am. Ceram. Soc.* **46**, 294 (1963).

⁴⁹ N. T. McDevitt, *J. Opt. Soc. Am.* **57**, 834 (1967).

⁵⁰ A. S. Barker, *Phys. Rev.* **132**, 1474 (1963).

⁵¹ R. Marshall and S. S. Mitra, *J. Chem. Phys.* **43**, 2893 (1965).

⁵² B. Piriou and F. Cabannes, *Compt. Rend.* **264B**, 1110 (1967).

⁵³ V. A. Kolesova, *Opt. i. Spektroskopiya* **6**, 38 (1959) [English transl.: *Opt. Spectry. (USSR)* **6**, 20 (1959)].

⁵⁴ K. Nakamoto, *Infrared Spectra of Inorganic and Coordination Compounds* (John Wiley & Sons, Inc., New York, 1963), p. 107.

purities¹⁰ in the tetrahedral sites of $Y_3Fe_5O_{12}$, where $920 < \bar{\nu} < 860 \text{ cm}^{-1}$. The SiO_4 tetrahedral frequencies^{54,55} in garnet are approximately $\bar{\nu}_3 = 890$ and $\bar{\nu}_4 = 500 \text{ cm}^{-1}$. The somewhat lower AlO_4 frequencies can be explained by the larger Al-O separation of 1.76 \AA compared to the Si-O separation^{41,56} of 1.64 \AA even though the atomic masses of Al and Si are nearly alike.

The conclusion is that the absorption peaks in Fig. 2 at $\bar{\nu} = 700, 729, 792 \text{ cm}^{-1}$ are components of the $\bar{\nu}_3$ vibration of the AlO_4 molecular groups at $\bar{\nu}_3 \sim 730 \text{ cm}^{-1}$ as split¹⁰ either by the low-symmetry crystal field of the garnet or by interactions with other molecular groups in the crystal. Each of these peaks of an "internal" vibration of YAG is still, of course, one of the 17 infrared-active T_{1u} modes of the YAG crystal. The weaker absorption at $\bar{\nu} = 820 \text{ cm}^{-1}$ in Table I and Fig. 2 has no definite assignment except that it is associated with the AlO_4 groups. A similar absorption shoulder occurs in the natural garnets.^{10,55} The three main lines of the $\bar{\nu}_3$ tetrahedral vibration also occur in the absorption spectra¹¹ of $Y_3Ga_5O_{12}$, $Y_3Fe_5O_{12}$, and also in⁴⁹ $Ho_3Fe_5O_{12}$, where they are presumably caused by the GaO_4 and FeO_4 groups in the lattice. The average $\bar{\nu}_3$ frequency is now about 600 cm^{-1} because of the larger size⁴¹ and mass of the Ga or Fe. The absorption band in Fig. 2 that corresponds to the $\bar{\nu}_4$ vibration of the AlO_4 group is not known. It may occur at $\sim 460 \text{ cm}^{-1}$, based on an analysis of the multiphonon portion of the spectrum (see below).

A further comparison of YAG with other crystals is also possible for the very lowest wave-number mode at $\bar{\nu} = 123 \text{ cm}^{-1}$. In the crystals $Dy_3Al_5O_{12}$, $Ho_3Al_5O_{12}$, and $Er_3Al_5O_{12}$, where Y is replaced by a rare-earth ion^{54,57}, this mode shifts to $\bar{\nu} = 95 \text{ cm}^{-1}$. It shifts further⁵⁸ to $\bar{\nu} = 85 \text{ cm}^{-1}$ for $Er_3Ga_5O_{12}$ and $Yb_3Ga_5O_{12}$. Here the Al has been replaced by Ga. This lowest mode in YAG thus appears to involve both the Y and Al ions, and is probably an external mode of the whole lattice.

Two-Phonon and Three-Phonon Region

The end of the one-phonon region is taken at $\bar{\nu} = 860 \text{ cm}^{-1}$. The absorption in Fig. 2 in the region $860 < \bar{\nu} < 2400 \text{ cm}^{-1}$ is believed to be caused by multiphonon processes in which one photon generates two or more phonons. The various peaks and their tentative assignments are given in Table II. These assignments have been made primarily on the basis of matching observed and calculated $\bar{\nu}$ values with some weight given to the intensity of the corresponding one-phonon peaks. It is not strictly correct to take the $\bar{\nu}$ values of Table I which are for phonons at $\mathbf{k} = 0$ in the Brillouin zone and assume that the zone boundary phonons that are

TABLE II. Tentative assignments of the multiphonon optical absorption bands observed in $Y_3Al_5O_{12}$ at 300°K .

$\bar{\nu}$, cm^{-1} observed	α cm^{-1}	Assignment	$\bar{\nu}$, cm^{-1} calculated	Suggested assignment
900	50	457+457	914	$\Sigma \nu_4$
975	2.1	457+510	967	
1028	1.6	457+570	1027	
1102	1.1	530+570	1100	
1245	7.0	457+784	1241	$\bar{\nu}_3 + \nu_4$
1295 \pm 5	4.5	510+784	1294	
1395 \pm 5	6.8	690+690 or 690+722	\sim 1395	$\Sigma \bar{\nu}_3$
1435	7.2	722+722	1444	
1460	7.2	690+784	1474	
1500	6.0	722+784	1506	
1530	5.4	690+830	1520	
1600	2.0	784+830	1614	
1680	0.35	830+830	1660	
2120	0.7	(3/2)(690+722)	2118	

involved in the multiphonon bands are identical in wave number. However, the change in $\bar{\nu}$ across the zone may be quite small because of the small intervals between modes and the small values of \mathbf{k} at the zone boundary. Therefore the assignments in Table II are meant to be suggestive rather than definitive. With the assignments made the two-phonon processes give rise to α values about 10^{-2} times as large as the one-phonon processes, while the three-phonon processes give α values about 10^{-4} times as large. The two-phonon processes produce an absorption peak in YAG at $\bar{\nu} = 1450 \text{ cm}^{-1}$ (see Fig. 2) which occurs at just about $2\bar{\nu}_3$. The three-phonon processes produce the peak at $\bar{\nu} = 2120 \text{ cm}^{-1}$, which is nearly equal to $3\bar{\nu}_3$ of the AlO_4 vibration. This peak at $\bar{\nu} = 2120 \text{ cm}^{-1}$ is an intrinsic feature of YAG and is not caused by trace impurities. It has also been seen by Cockayne.³ Wood and Remeika⁵⁸ have also seen the $2\bar{\nu}_3$ and $3\bar{\nu}_3$ peaks of the FeO_4 groups in $Y_3Fe_5O_{12}$ at $\bar{\nu} = 1200$ and $\sim 1700 \text{ cm}^{-1}$.

The assignments in Table II also indicate that the AlO_4 mode at $\bar{\nu}_3$ does not couple very strongly to any of the lower wave-number modes $0 < \bar{\nu} < 620 \text{ cm}^{-1}$ except the two modes at $\bar{\nu} = 457$ and 510 cm^{-1} . These two modes may therefore be components of the $\bar{\nu}_4$ mode of the AlO_4 groups. Similarly the four peaks at $\bar{\nu} = 900, 975, 1028, 1102 \text{ cm}^{-1}$ may be two-phonon peaks of the $\bar{\nu}_4$ mode of AlO_4 . This assignment of the absorption region $457 \leq \bar{\nu} \leq 570$ to the $\bar{\nu}_4$ mode of AlO_4 is very uncertain, and requires further work to either justify or alter the assignment. The two-phonon (and three-phonon) absorption bands associated with the one-phonon peaks for $123 \leq \bar{\nu} \leq 395 \text{ cm}^{-1}$ will be masked by the much stronger one-phonon (and two-phonon) peaks at higher wave numbers, and so are not seen.

FUNDAMENTAL ABSORPTION EDGE

The results for the fundamental absorption-edge region where $30\,000 < \bar{\nu} < 55\,000 \text{ cm}^{-1}$ are shown in

⁵⁴ J. M. Hunt, M. P. Wisherd, and L. C. Bonham, *Anal. Chem.* **22**, 1478 (1950).

⁵⁵ S. C. Abrahams and S. Geller, *Acta Cryst.* **11**, 437 (1958).

⁵⁷ D. L. Wood and J. P. Remeika, *J. Appl. Phys.* **38**, 1038 (1967).

⁵⁸ A. J. Sievers and M. Tinkham, *Phys. Rev.* **129**, 1995 (1963).

TABLE III. Single crystals of $Y_3Al_5O_{12}$ used in the study of the optical absorption in the ultraviolet region, $\bar{\nu} > 30\,000\text{ cm}^{-1}$. SRF=standard radio-frequency heating conditions, in which a thick-wall (0.15-cm) iridium crucible is directly heated with a 450-kc/sec rf generator. SM=stoichiometric melt of $3.000Y_2O_3 + 5.000Al_2O_3$. Linde=crystal obtained from Union Carbide Corporation* in 1965. The other crystals were grown in this laboratory between Oct. 1966 and March 1968.

Crystal number	Atmosphere during growth	Comments
B26	Helium	tungsten susceptor +Ir crucible, SM
Linde	?	Ir crucible
M4	Argon	tungsten susceptor +Ir crucible, SM
M9	A+0.2% O_2	SRF, SM
M12	A+0.5% O_2	SRF, SM
M15	A+0.5% O_2	SRF, 3.000 Y_2O_3 +5.002 Al_2O_3 melt
M18	A+0.5% O_2	SRF, 3.005 Y_2O_3 +5.000 Al_2O_3 melt
M28	A+0.1% O_2	SRF, SM

* Reference 36.

Fig. 3. Here the absorption curves for $\alpha < 10\text{ cm}^{-1}$ vary from sample to sample; see Table III. However, for $\alpha > 10\text{ cm}^{-1}$ all of the crystals are identical, and show a steeply rising edge which is believed to be the fundamental absorption edge. The coefficient α reaches a value of 10^3 cm^{-1} at $\bar{\nu} = 54\,300\text{ cm}^{-1}$ ($\lambda = 0.184\ \mu$ or $h\nu = 6.73\text{ eV}$).

The variation in α from sample to sample in the range $30\,000 < \bar{\nu} < 52\,000\text{ cm}^{-1}$ appears to depend on the purity and/or the growing conditions of the crystal. It does not appear to depend on the stoichiometry of the melt. Crystal M12 was grown from a nearly exact $3Y_2O_3$ -to- $5Al_2O_3$ melt. Then small additions of Al_2O_3 or Y_2O_3 were made to the same melt and crystals M15 (see Fig. 3 caption) and M18, respectively, were grown. No difference in α values was found, as can be seen from Fig. 3. Cockayne³ found substantial changes in α for what must have been much larger variations in stoichiometry.

Crystal M28 has the lowest α values in this region. It was also found to be particularly clear, and free of Tyndall scattering centers in the visible part of the spectrum where $15\,000 < \bar{\nu} < 20\,000\text{ cm}^{-1}$. The variable, residual optical absorption in the $30\,000 < \bar{\nu} < 52\,000\text{ cm}^{-1}$ region is probably caused by random variations from run to run in the impurity concentration in the range of 10 to 100 ppm. The impurities give rise to what might be called two absorption bands centered about $\bar{\nu} = 39\,000$ and $45\,000\text{ cm}^{-1}$. These occur in the same wave-number range as the absorption tail found by O'Bryan and O'Connor² in floating-zone-grown $Y_3Al_5O_{12}$. They do not correspond in energy to the color-center absorption band found by Bass and Paladino²² at $\bar{\nu} = 30\,800\text{ cm}^{-1}$. The exact cause of this variable absorption in the ultraviolet is uncertain.

COMMENTS ON YAG AS A HOST CRYSTAL

Single crystals of YAG, as mentioned earlier, serve as a host in the study of the optical absorption or luminescence of many transition-metal and rare-earth-metal ions. In either case the ions possess certain optical transitions associated with the d -shell or f -shell electrons. In these transitions a zero-phonon line is usually present, and this is often accompanied by sidebands which are due to phonon-assisted transitions. Here a transition between two distinct electronic levels occurs simultaneously with the emission (or absorption) of one or more lattice phonons. The characteristic wave numbers of the phonons involved will usually be those for which the phonon density of states exhibits a local maximum. Thus the phonon wave numbers will not be exactly those listed in Table I, but should be closely similar for the same reasons as given in the section entitled Two-Phonon and Three-Phonon Region.

Identification of YAG Modes

For many impurity ions it is known into which of the three different cation sites the impurity will be incorporated. Thus the phonon sidebands may yield information about which modes of YAG are coupled to that particular lattice site. For example, Yb^{3+} enters the Y^{3+} site. The results of Buchanan *et al.*³⁰ on the phonon sidebands of Yb^{3+} in YAG and $Yb_3Al_5O_{12}$ show that the phonons involved cover the wave-number range $100 < \bar{\nu} < 580\text{ cm}^{-1}$. No sidebands were seen in the range $620 < \bar{\nu} < 860\text{ cm}^{-1}$. This result agrees with our interpretation that the $620 < \bar{\nu} < 860\text{ cm}^{-1}$ range in Fig. 2 is associated with the AlO_4 groups and does not involve the Y ions. The only modes involving Y must therefore lie in the range $100 < \bar{\nu} < 580\text{ cm}^{-1}$.

Chromium Cr^{3+} impurities enter the YAG lattice on the octahedral sites and give rise to a strong luminescence.¹²⁻¹⁶ In particular, the R -line luminescence has a pronounced, characteristic phonon sideband on its low-energy side^{13,14,16} from 4 to 300°K . Both the $100 < \bar{\nu} < 620\text{ cm}^{-1}$ and $620 < \bar{\nu} < 860\text{ cm}^{-1}$ phonon regions can be seen, although the former is much stronger than the latter. The 4°K spectrum¹⁴ shows discrete phonon energies of $\bar{\nu} = 128, 143, 164, 182, 199, 219$, etc. (as read from the photograph). Four of these occur in Table I. This sideband of the R lines is thus caused by phonons and not by Cr pairs, as the authors¹⁴ had suggested. Furthermore, the Cr^{3+} ions apparently couple to the external lattice modes as well as to the internal AlO_4 modes, although the coupling to the AlO_4 group $\bar{\nu}_3$ modes is weak.

Electronic Levels of Rare-Earth Ions

A knowledge of the lattice-vibration spectrum of $Y_3Al_5O_{12}$ can be very useful in interpreting the optical spectra of rare-earth ions dissolved in $Y_3Al_5O_{12}$ as a host crystal. Buchanan *et al.*³⁰ have shown that Yb^{3+}

ions in $Y_3Al_5O_{12}$ have very pronounced phonon sidebands, and care must be exercised in separating these pure electronic transitions from the phonon-assisted sidebands of such transitions. Previous work by Wood²⁰ on Yb^{3+} in $Y_3Al_5O_{12}$ assigned levels at $\bar{\nu}=140$ and 490 cm^{-1} to the Yb^{3+} ground-state manifold. These are now known to be incorrect.³⁰ Allowing for some shifts in wave number they probably correspond to strong lattice modes near $\bar{\nu}=123$ and 463 cm^{-1} . The electronic level at $\bar{\nu}=620\text{ cm}^{-1}$ found by Wood²⁰ does appear to be the 611 cm^{-1} one found by Buchanan *et al.*³⁰ Similarly the level at $\bar{\nu}=388\text{ cm}^{-1}$ for Yb^{3+} in $Y_3Al_5O_{12}$ postulated by Koningstein²⁴ may well be caused by the strong lattice doublet near $\bar{\nu}=377$, and 397 cm^{-1} .

The levels of the ground-state manifold of Er^{3+} in $Y_3Ga_5O_{12}$, $Er_3Al_5O_{12}$, and $Er_3Ga_5O_{12}$ are now well known.^{57,59-62} For Er^{3+} in $Er_3Al_5O_{12}$ the first five levels of the $^4I_{15/2}$ manifold occur at $\bar{\nu}=0, 26.6, 58.4, 78.8$ and 422.8 cm^{-1} , and they should be very similar for Er^{3+} in $Y_3Al_5O_{12}$. Thus the assignment of Koningstein and Geusic²³ of $\bar{\nu}=0, 24, 72, 116, 412\text{ cm}^{-1}$ for this ion appears to be incorrect. They appear to have missed the level at $\bar{\nu}=58\text{ cm}^{-1}$, and the $\bar{\nu}=116\text{ cm}^{-1}$ assignment may be that of a lattice mode of $Y_3Al_5O_{12}$ near $\bar{\nu}=123\text{ cm}^{-1}$.

The present data on the optically active lattice modes of $Y_3Al_5O_{12}$ should be of assistance in helping to unravel the competition between electronic and phonon-assisted transitions in various rare-earth ion spectra.

CONCLUSIONS

The optical absorption of $Y_3Al_5O_{12}$ shows a broad lattice phonon absorption region extending from $100 < \bar{\nu} < 2400\text{ cm}^{-1}$. The $100 < \bar{\nu} < 860\text{ cm}^{-1}$ region corresponds to one-phonon transitions while two- and three-phonon processes dominate from $860 < \bar{\nu} < 2400\text{ cm}^{-1}$. The absorption in the region $620 < \bar{\nu} < 860\text{ cm}^{-1}$

⁵⁹ R. Pappalardo, *Z. Physik* **173**, 374 (1963).

⁶⁰ B. Dreyfus, J. Verdone, M. Veyssie, *J. Phys. Chem. Solids* **26**, 107 (1965).

⁶¹ K. G. Kellwege, S. Huefner, M. Schinkmann, and H. Schmidt, *Phys. Kondensierten Materie* **4**, 397 (1966).

⁶² H. M. Crosswhite and H. W. Moos, in *Optical Properties of Ions in Crystals* edited by H. M. Crosswhite and H. W. Moos, (Interscience Publishers, Inc., New York, 1967), p. 3.

appears to be associated with AlO_4 groups in the lattice. In the region $2400 < \bar{\nu} < 30\,000\text{ cm}^{-1}$ the $Y_3Al_5O_{12}$ is optically transparent and $\alpha < 0.1\text{ cm}^{-1}$. At higher energies there is a region of weak, variable absorption depending on sample purity for $30\,000 < \bar{\nu} < 52\,000\text{ cm}^{-1}$. The fundamental absorption rises rapidly for $\bar{\nu} > 52\,000\text{ cm}^{-1}$ up to α values of at least 10^4 cm^{-1} . In the absorption-edge region $\alpha \geq 10^8\text{ cm}^{-1}$ for $\bar{\nu} \geq 54\,300\text{ cm}^{-1}$.

These results should be useful both for understanding $Y_3Al_5O_{12}$ and for the interpretation of the spectra of various rare-earth and transition-metal ions in $Y_3Al_5O_{12}$ as a host.

Note added in manuscript. After the preparation of this manuscript, a preprint of a paper⁶³ by J. P. Hurrell *et al.* was received in which the optical phonons in YAG were studied by reflectivity and Raman scattering. They found 15 of the 17 infrared-active modes at nearly the same wave numbers as reported here. The k values at the absorption peaks are generally larger than those found here (see Fig. 4). This may, in part, be a consequence of the fact that the k values for the more intensely absorbing peaks in Fig. 4 are derived from powder spectra.

Note added in proof. The α versus $\bar{\nu}$ curve for a flux grown crystal of YAG from Airtron, Morris Plains, N. J. was measured. It was colorless and transparent in the visible but possessed a broad absorption peak at $\bar{\nu}=38\,000\text{ cm}^{-1}$, where $\alpha=35\text{ cm}^{-1}$. This impurity absorption region merged with the intrinsic edge at $\bar{\nu}=52\,500\text{ cm}^{-1}$, where $\alpha=150\text{ cm}^{-1}$, see Fig. 3.

ACKNOWLEDGMENTS

The authors would like to thank J. H. McTaggart and G. Brower for much painstaking work in growing the crystals of $Y_3Al_5O_{12}$ and J. H. McTaggart for his help in preparing the crystals for the optical measurements. They also wish to thank Dr. M. C. M. O'Brien for her aid in understanding the group theory and allowed optical transitions in YAG, and L. C. Kravitz for information on the Raman scattering.

⁶³ J. P. Hurrell, S. P. S. Porto, I. F. Chang, S. S. Mitra, and R. P. Bauman, *Phys. Rev.* **173**, 851 (1968).